

Chapter 8: Solar and stellar magnetic activity

The role of complex magnetic topologies on stellar spin-down

Victor Réville¹, Allan Sacha Brun¹, Antoine Strugarek^{2,1}, Sean P. Matt³, Jérôme Bouvier⁴, Colin P. Folsom⁴ and Pascal Petit⁵

¹Laboratoire AIM, DSM/IRFU/SAP, CEA Saclay, email: victor.reville@cea.fr

²Département de physique, Université de Montréal

³Department of Physics and Astronomy, University of Exeter

⁴IPAG, Université Joseph Fourier Grenoble

⁵IRAP, CNRS - Université de Toulouse

Abstract. The rotational braking of magnetic stars through the extraction of angular momentum by stellar winds has been studied for decades, leading to several formulations. We recently demonstrated that the dependency of the braking law on the coronal magnetic field topology can be taken into account through a simple scalar parameter: the open magnetic flux. The Zeeman-Doppler Imaging technique has brought the community a reliable and precise description of the surface magnetic field of distant stars. The coronal structure can then be reconstructed using a potential field extrapolation, a technique that relies on a source surface radius beyond which all field lines are open, thus avoiding a computationally expensive MHD simulations. We developed a methodology to choose the best source surface radius in order to estimate open flux and magnetic torques. We apply this methodology to five K-type stars from 25 to 584 Myr and the Sun, and compare the resulting torque to values expected from spin evolution models.

Keywords. stars: coronae, rotation, magnetic fields, low-mass, mass loss

1. Introduction

For almost 20 years, Zeeman-Doppler Imaging (Donati & Brown 1997) has given us access to the surface magnetic field of active stars. Observations have confirmed the bonds between rotation, magnetism and evolution of solar-like stars, stars that are able to generate magnetic fields through dynamo processes in their convective envelope (Bouvier *et al.* 1997; Irwin & Bouvier 2009; Reiners & Mohanty 2012; Vidotto *et al.* 2014).

The rotational evolution of such stars are also driven by their winds, outflows generated in the alfvén wave heated coronae, that expand and carry away angular momentum. Wind braking has been studied for decades (Parker 1958; Schatzman 1962; Weber & Davis 1967; Kawaler 1988; Matt *et al.* 2012), and several scaling laws have been shown to reproduce the observations of rotation rates (Gallet & Bouvier 2013; Matt *et al.* 2015). In Réville *et al.* (2015a), we derived a formulation able to account for the complexity of the magnetic field using a simple scalar parameter: the unsigned open magnetic flux. However, the open magnetic flux is not yet observable and is a result of the coronal structure and wind properties, which can only be recovered through models.

Réville *et al.* (2015b) propose a simple model to compute the open flux using a potential field extrapolation and a wisely chosen source surface radius, thus avoiding more time consuming MHD simulations. Here, we apply this model to several targets, K-type stars whose age vary from 25 to 584 Myr and the Sun and compare the torque we obtain with spin evolution models.

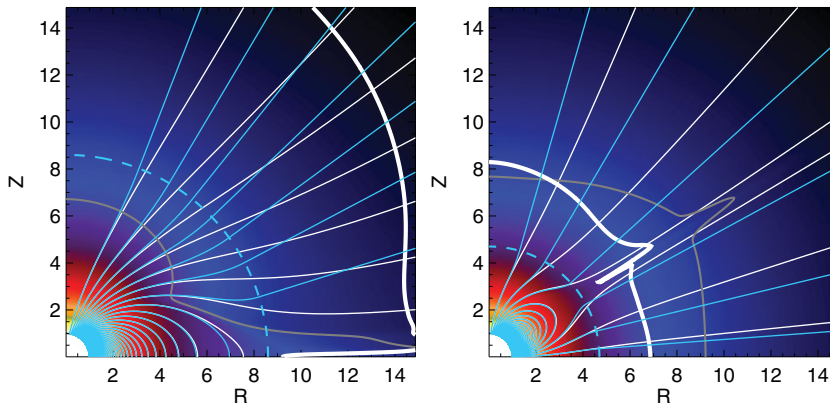


Figure 1. Comparison of wind simulations and potential field extrapolations with the optimal source surface in a dipolar and a quadrupolar case. The thin white field lines are the magnetic field lines from the simulation while the cyan lines are from the potential field extrapolation. The thick white line is the Alfvén surface and the thick cyan dashed line is the optimal source surface.

2. Potential field extrapolation with an optimal source surface

The potential field source surface model has been used extensively in solar physics to easily recover the structure of the corona. This model assumes no currents between the surface of the star and the spherical source surface, whose radius has been often set around a fiducial value of $2.5R_{\odot}$. This value is the only free parameter of the model given the surface magnetic field of the Sun and it has been chosen to match the polarity of the radial magnetic field observed by spacecrafts at 1 A.U (Hoeksema *et al.* 1983). Beyond this surface, the field is completely radial to mimic the opening of the field lines by the wind. The total flux is thus constant beyond this radius. Recently, this value has been proposed to vary over the 11-year solar cycle (Lee *et al.* 2011; Arden *et al.* 2014) to account for change in the solar magnetic field. Hence in order to apply this model to other stars, whose surface magnetic field is now within reach thanks to Zeeman Doppler imaging, and has been shown to reach the kilogauss scale, the best source surface must be chosen wisely.

We chose to rely on the 60 wind simulations we performed in Réville *et al.* (2015a) to find an optimal source surface radius that matches the open magnetic flux of the simulation. The optimal source surface $r_{ss,opt}$ is thus defined as the zero of the function:

$$F(r_{ss}) = \Phi_{open}(r_{ss}) - \Phi_{open,sim}. \quad (2.1)$$

We find that the optimal source surface radius varies as a function of the magnetic field strength, the magnetic field topology and the rotation rate (see Réville *et al.* 2015b, for a detailed study). Figure 1 shows a comparison of the simulation and the potential field extrapolation obtained with the optimal source surface. We see that the size of the streamers is well reproduced by the potential field extrapolation in both cases. The optimal source surface radius corresponds to the size of the largest streamer in the simulation and is different from 2.5 stellar radii. However, the potential field extrapolation deviates from the wind solution beyond the source surface, due to its constraint to have a purely radial field there, whereas the field from the simulation takes more distance to reach radially (see Riley *et al.* 2006; Cohen 2015, for an extended comparison of potential extrapolations and MHD simulations). This should raise attention to the use of potential

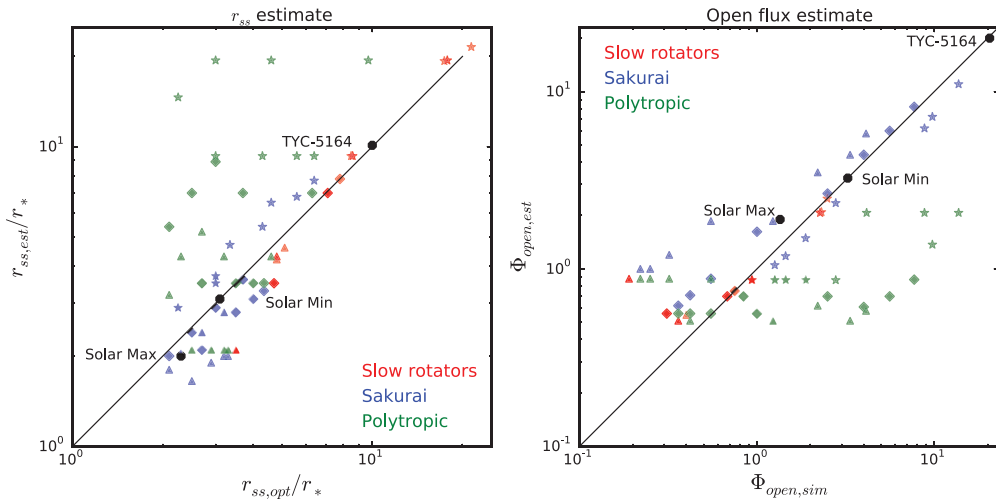


Figure 2. Comparison between the estimated and the optimal source surface radius (left panel) and the resulting estimation of the open flux (right panel). Slow rotators are marked in red, given that both wind models yield the same results. The difference is apparent for fast rotators ($f \geq 0.01$) where green points are obtained with the polytropic wind model, and the blue points are obtained with the Sakurai wind model. The symbols stand for the topology of the magnetic field, stars for dipoles, diamonds for quadrupoles and triangles for octupoles.

field extrapolation to compute expansion factors in solar wind models, or the coronal properties of the magnetic field (Wang & Sheeley 1990; Titov *et al.* 2012).

3. Open flux calculations using an estimate of the optimal r_{ss}

In order to compute the coronal structure of a given star and its open flux, without any MHD simulation, we propose a method to estimate the optimal source surface. We compare the hydrodynamical pressure (thermal pressure and ram pressure) of two spherically symmetric wind models to the magnetic pressure of the multipolar expansion of the surface magnetic field. We assume that the source surface radius is the averaged spherical radius where the equality of those pressures is reached:

$$P_{hydro} = p + \rho v^2 = \frac{B^2}{2\mu_0} = P_{mag}, \text{ at } r = r_{ss} \quad (3.1)$$

where p, ρ and v are the pressure, density and velocity profile computed with the wind model, and B the extrapolated magnetic field.

We used a polytropic wind model with $\gamma = 1.05$ -the value we use in our simulations-, and a more elaborated wind model that includes the effect of the magneto-centrifugal acceleration. This model was introduced by Weber & Davis (1967) and conveniently formalized by Sakurai (1985). More details about the implementation are given in Réville *et al.* (2015b). The results we get for the estimation of the source surface radius and the open flux are given in Figure 2.

The estimations we get with this method are satisfying for slow rotators and fast rotators using the Sakurai wind model. In the case of fast rotators, the magneto-centrifugal effect can be the dominant process in the wind acceleration, this is why the polytropic model cannot capture correctly the structure of the coronal loops in this case. Details and discussion about the caveats of this model are given in Réville *et al.* (2015b).

4. Torque calculation methodology

We use the formulation we provide in Réville *et al.* (2015a):

$$\tau_w = \dot{M}_w^{1-2m} \Omega_* R_*^{2-4m} K_3^2 \left(\frac{\Phi_{open}^2}{v_{esc}(1+f^2/K_4^2)^{1/2}} \right)^{2m}, \quad (4.1)$$

where τ_w is the torque applied by the wind to the star, \dot{M}_w is the mass-loss rate due to the wind, R_* , Ω_* , $f \equiv \Omega_* R_*^{3/2} (GM_*)^{-1/2}$, v_{esc} are the stellar radius, the stellar rotation rate, the break-up ratio and the escape velocity. The constants values are $K_3 = 0.64$, $K_4 = 0.06$, and $m = 0.3$ †.

The open flux can now be estimated using the method described above, using for instance a spectropolarimetric map of the surface magnetic field and the usual stellar parameters (Ω_* , R_* , M_*). However, the wind models rely on two additional parameters that are the coronal base density and temperature. We used the prescriptions given in Holzwarth & Jardine (2007) to estimate those parameters as a function of the rotation rate of the star:

$$T = T_\odot \left(\frac{\Omega_*}{\Omega_\odot} \right)^{0.1}, \quad n = n_\odot \left(\frac{\Omega_*}{\Omega_\odot} \right)^{0.6}. \quad (4.2)$$

$T_\odot = 1.5 \times 10^6$ K and $n_\odot = 10^8$ cm⁻³ are calibrated such that a polytropic wind with $\gamma = 1.05$ recover a wind velocity of 444 km.s⁻¹ at 1 A.U and a mass-loss rate of $3.2 \times 10^{-14} M_\odot$ /yr. The torque calculation can be then performed in the following steps:

- (a) Compute the wind pressure, velocity and density profiles.
- (b) Compute the mass-loss rate using the simple assumption that $\dot{M}_w = 4\pi\rho v^2 r^2$.
- (c) Find the estimate for the source surface radius through pressure balance.
- (d) Compute the potential extrapolation from the spectropolarimetric map with the estimated source surface and extract the open flux (here we use only the radial field B_r to perform the extrapolation).
- (e) Compute the torque following Réville *et al.* (2015a).

5. Application

We apply this methodology to five stars varying in age as well as the Sun in the minimum and maximum state of activity during cycle 22. The surface magnetic field were observed thanks to the two spectropolarimeters NARVAL at the TBL (Télescope Bernard Lyot) and ESPaDOnS at the CFHT (Canada France Hawaii Telescope) (Folsom *et al.* 2016). The Sun magnetic maps were obtained at the Wilcox observatory (DeRosa *et al.* 2012). The properties of those stars are given in the following Table:

Name	Age (Myr)	Period (days)	Mass (M_\odot)	Radius (R_\odot)	T_{eff} (K)	$\langle B_r \rangle$ (G)
BD 16351	27	3.3	0.9	0.9	5243	33
TYC 5164-567-1	120	4.7	0.85	0.85	5130	48.8
HII 296	125	2.6	0.9	0.9	5322	52
DX Leo	257	5.4	0.9	0.9	5354	21.3
AV 2177	584	8.4	0.9	0.9	5316	5.4
Solar Min	4570	28	1.0	1.0	5778	1.1
Solar Max	4570	28	1.0	1.0	5778	2.6

† A mistake was made in Réville *et al.* (2015a), where all the values of Φ_{open} should have been multiplied by $\sqrt{4\pi}$, thus changing the K_3 constant value from 1.4 to 0.64.

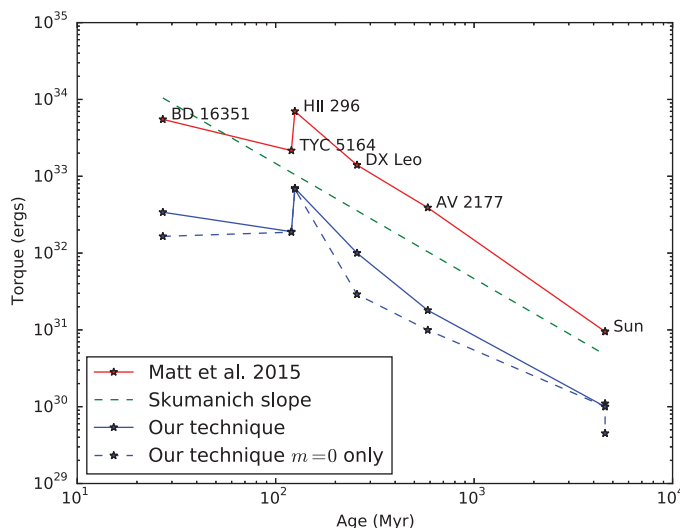


Figure 3. Comparison of the torque obtained with our technique with the empirical torque formulation of Matt *et al.* (2015) (red line). We either used the full spectropolarimetric map (plain blue line) or only the axisymmetric components of the magnetic field (dashed blue line). The Skumanich’s law slope: $\tau_w \propto t^{-3/2}$ (Skumanich 1972, showed that $\Omega_* \propto t^{-1/2}$ and for non-saturated stars: $\tau_w \propto \Omega_*^3$), fits the slowest rotators, but not the saturated regime, while red and blue curves do.

The resulting torques are given in Figure 3. We take as a comparison the torque formulation given in Matt *et al.* (2015) that is calibrated to reproduce clusters observation. Assuming a dynamo saturation threshold of $10 \Omega_\odot$, the equation for this torque are:

$$\tau_w = -\tau_{w,0} \left(\frac{\tau_{cz}}{\tau_{cz,0}} \right)^2 \left(\frac{\Omega_*}{\Omega_\odot} \right)^3 \text{ (unsaturated), } \tau_w = -10^2 \tau_{w,0} \left(\frac{\Omega_*}{\Omega_\odot} \right) \text{ (saturated),} \quad (5.1)$$

where:

$$\tau_{w,0} = 9.5 \times 10^{30} \text{ erg} \left(\frac{R_*}{R_\odot} \right)^{3.1} \left(\frac{M_*}{M_\odot} \right)^{0.5}. \quad (5.2)$$

We apply our technique using the full spectropolarimetric map, but also only the axisymmetric components of the magnetic field. We find that our technique shows a systematic offset with the spin down model value. This offset is not new and also exists in the previous work of Matt *et al.* (2012); Matt & Pudritz (2008), since our formulation is equivalent in the dipolar case. The solar calibration of this model seems to be fully responsible for this offset. There are many possible reasons for it, starting with an improvement of the physics modeling in our wind simulations, leading to a better understanding of the parameters we use for this simple model. How can we understand the value of n_\odot and T_\odot in the real solar wind, subject to volumetric heating, and complex terminal speed distribution? The time variability of the Sun is also likely to be an answer, a more active Sun in the past could explain the statistical value of the torque we need to use to reproduce the observations.

However, when the full spectropolarimetric map is used, the slope and variation of the torque are well reproduced. Thus, the evolution of the stellar parameters as a function of stellar rotation seems reliable, and is coherent with the magnetic field amplitude we get from ZDI maps. Also, it is likely that the non-axisymmetric modes also contribute to the

wind braking even though our torque formulation was computed with an axisymmetric setup.

6. Conclusions

Our technique is able to reproduce the trend of the angular momentum loss with time that is expected from the evolution of observed spin rates, but with a systematic underestimation. Many reasons can be invoked for this difference, given the hypothesis both approach assumed. In our case, our torque formulation was computed with an axisymmetric setup, in ideal MHD, with a constant γ and coronal temperature for the wind. Exploring the influence of more complex models for the wind, including for instance, resistive MHD, heating terms in the low-corona and studying the influence of slow and fast streams could improve this formulation. A preliminary study indicates that, with different γ , a torque 3 times higher in the Solar case can be reached, hence bringing closer our approach to spin evolution models that have their own limitations.

For instance, the answer might be in the time variability of the stellar magnetic activity. We have taken here snapshots of the surface magnetic field of those stars, and our method is calibrated on the current state of the Sun while the relevant timescales for the evolution of spin rate are of the order of $10^6 - 10^9$ years.

This simple technique is, nonetheless, a powerful tool to drive the future theoretical improvements. It can also be used with care to infer wind properties of other stars and better constrain their mass-loss.

References

- Arden, W. M., Norton, A. A., & Sun, X. 2014, *JGR (Space Physics)*, 119, 1476
 Bouvier, J., Forestini, M., & Allain, S. 1997, *A&A*, 326, 1023
 Cohen, O. 2015, *Solar Physics*, arXiv:1507.00572
 DeRosa, M. L., Brun, A. S., & Hoeksema, J. T. 2012, *ApJ*, 757, 96
 Donati, J.-F. & Brown, S. F. 1997, *A&A*, 326, 1135
 Folsom, C. P., Petit, P., Bouvier, J., *et al.* 2016, *MNRAS*, 457, 580
 Gallet, F. & Bouvier, J. 2013, *A&A*, 556, A36
 Hoeksema, J. T., Wilcox, J. M., & Scherrer, P. H. 1983, *JGR*, 88, 9910
 Holzwarth, V. & Jardine, M. 2007, *A&A*, 463, 11
 Irwin, J. & Bouvier, J. 2009, in IAU Symposium, Vol. 258, 363
 Kawaler, S. D. 1988, *The Astrophysical Journal*, 333, 236
 Lee, C. O., Luhmann, J. G., Hoeksema, J. T., *et al.* 2011, *Solar Physics*, 269, 367
 Matt, S. & Pudritz, R. E. 2008, *ApJ*, 678, 1109
 Matt, S. P., Brun, A. S., Baraffe, I., Bouvier, J., & Chabrier, G. 2015, *ApJL*, 799, L23
 Matt, S. P., Pinzón, G., Greene, T. P., & Pudritz, R. E. 2012, *ApJ*, 745, 101
 Parker, E. N. 1958, *ApJ*, 128, 664
 Reiners, A. & Mohanty, S. 2012, *ApJ*, 746, 43
 Réville, V., Brun, A. S., Matt, S. P., Strugarek, A., & Pinto, R. F. 2015a, *ApJ*, 798, 116
 Réville, V., Brun, A. S., Strugarek, A., *et al.* 2015b, *Accepted in ApJ*, arXiv:1509.06982
 Riley, P., Linker, J. A., Mikić, Z., *et al.* 2006, *ApJ*, 653, 1510
 Sakurai, T. 1985, *A&A*, 152, 121
 Schatzman, E. 1962, *Annales d'Astrophysique*, 25, 18
 Skumanich, A. 1972, *ApJ*, 171, 565
 Titov, V. S., Mikic, Z., Török, T., Linker, J. A., & Panasenco, O. 2012, *ApJ*, 759, 70
 Vidotto, A. A., Jardine, M., Morin, J., *et al.* 2014, *MNRAS*, 438, 1162
 Wang, Y.-M. & Sheeley, Jr., N. R. 1990, *ApJ*, 355, 726
 Weber, E. J. & Davis, Jr., L. 1967, *ApJ*, 148, 217